JOURNAL OF CATALYSIS 145, 501–507 (1994)

Field Emission Microscopy Study of Supported Bimetallic Catalysts Pd–Mo/Al_2O_3/W: Nitrogen Spillover

Jan Šotola and Zlatko Knor

J. Heyrovský Institute of Physical Chemistry and Electrochemistry, Academy of Sciences of the Czech Republic, 182 23 Prague 8, Czech Republic

Received March 26, 1993; revised July 26, 1993

Thin polycrystalline layers (clusters) of palladium and/or molybdenum were deposited onto a continuous layer of Al_2O_3 covering a tungsten field emitter. This sandwich system represents a realistic model for a supported metal catalyst. Investigation of nitrogen interaction with these systems at room temperature proved that there is spillover of nitrogen atoms from molybdenum to palladium.

1. INTRODUCTION

The differences in chemical properties of bulk metals and of supported metal clusters are often discussed in the literature (1–3). These differences are due to the different electronic structure of small isolated clusters in comparison with the bulk metal and/or to the metal–support interaction (3) (e.g., strong metal–support interaction, the so-called SMSI effect). We have recently tried to contribute to the solution of the general problem of the gap between real catalysis performed on supported metal catalysts and surface science studies on single crystals by realistic modeling of supported metal catalysts in the field emission microscope (FEM) (4, 5).

Formerly, a thin layer of tungsten oxide represented the support in our model system (4, 5). Recently, we extended our studies to a technologically important support, a thin alumina layer. This extension was made possible by the construction of a new UHV apparatus where the field emitter can be covered by at least three various components evaporated from optional directions.

In this study we report on the Mo–Pd bimetallic system deposited on alumina and its interaction with nitrogen at room temperature.

2. EXPERIMENTAL

The experiments were performed in a commercial stainless-steel UHV apparatus USU 4 (USSR provenance), further equipped with a turbomolecular pump (Balzers, Liechtenstein) and a sapphire leak valve (Varian) connected to the all-glass gas-handling system. The adsorption and reaction experiments were performed under dynamic conditions of gas dosing. The purity of gases was checked by a quadrupole mass spectrometer (Finnigan 400, USA).

The glass cold finger holding the loop with a spot-welded field emitter was mounted on a bellows enabling the tilting and shifting of the sample in front of the screen (Fig. 1). The screen can be shifted independently towards or away from the tip.

The evaporation sources of Mo, Pd, and Al were mounted onto a rotatable x, y, z-manipulator. The metal spirals of the evaporation sources are shielded in order to deposit the metal in the desired direction only (Fig. 1).

The tungsten tips were etched electrochemically in a solution of KOH and NH_4OH applying 2–5 V AC. The tips were cleaned by short flashing to about 2600 K in vacuo, the residual gas pressure being lower than 10^{-9} mbar.

The tip temperatures were determined by calibrating the heating currents through the tungsten loop with the use of an optical pyrometer. Pyrometer measurements were corrected to true temperatures by using reported emissivity values for tungsten. The error in the temperature estimation is about ± 50 K in the range 900–2600 K.

3. RESULTS AND DISCUSSION

3.1. Formation of the Pd–MO/Alumina System

Figure 2 shows the sequence of FEM images of: (i) a clean tungsten surface; (ii) an aluminum layer, evaporated onto the tungsten surface (successively from the front, the right and the left side); (iii) an oxidized aluminum layer (by exposing the Al layer for 30 s to 1×10^{-6} mbar of oxygen at the temperature of $T \approx 1250$ K; and (iv) palladium and molybdenum layers evaporated from the right and left sides, respectively.

Comparison of Figs. 2c and 2d–2g shows that the palladium and molybdenum clusters deposited on the alumina

0021-9517/94 $6.00

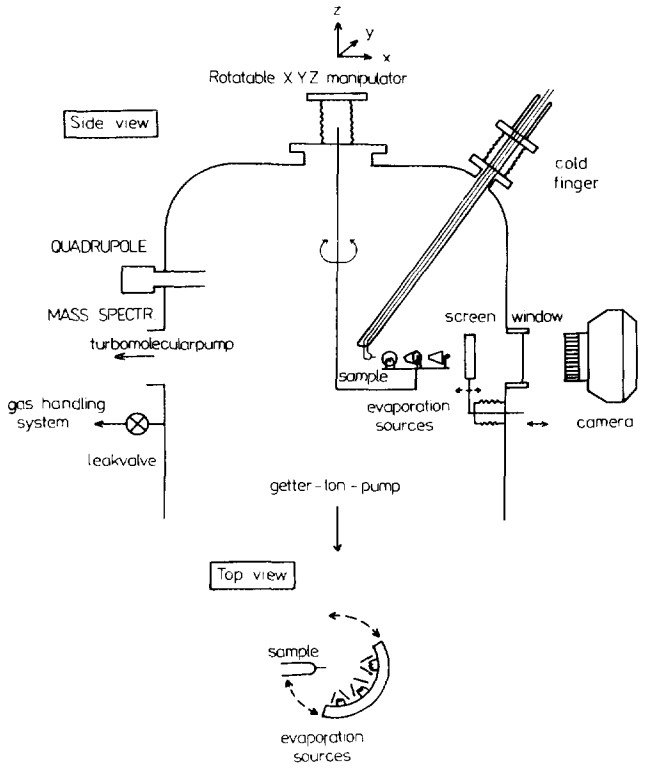

FIG. 1. Scheme of the apparatus.

layer are well visible. The aluminum oxide does not contribute to the emission current at voltages needed to image the metals. Thereafter, all the emission current changes can be related to the processes occurring on the metal clusters only.

Considering the conditions of the oxidation process, we presume the Al_2O_3 to be in the form of a polycrystalline layer of γ-alumina, about 1–2 nm thick (6). As reported by Chen *et al.* (6), there is no evidence of Mo diffusion through the alumina layer or formation of molybdenum oxide by heating up to 1300 K. We can therefore expect that neither the diffusion of underlying tungsten nor the transport of molybdenum overlayer (and possibly neither diffusion of palladium) through the alumina layer occurs, since the driving force for inward diffusion of Mo or Pd, viz., the presence of metallic aluminum (which is able to diffuse through the Al_2O_3 layer) is lacking.

If heated, molybdenum starts to evaporate earlier than palladium (Figs. 2e and 2f). The emission current from any particular surface region of this bimetallic system depends on the local radius of curvature, related to the thickness of the metal layer, as can be seen in Fig. 2f, where the amount of palladium was the same as in Fig. 2g and an additional dose of molybdenum was deposited.

The visibility and the behavior of Pd and Mo on alumina are actually very similar to their behaviour on the oxidized tungsten tips (7, 8). The essential difference in conductivity of tungsten oxide (semiconductor) and alumina (insulator) seems to be not very important for imaging of metal overlayers.

3.2. *Thermal Desorption of Al_2O_3 Layer*

Figure 3 shows the thermal desorption of the alumina layer from the tungsten tip. The layer starts to evaporate at about 1400 K (Fig. 3c) which allows us to conclude that up to 1300 K we can anneal or even evaporate the deposited molybdenum or palladium layer without destroying the underlying alumina support.

The character of the thermal desorption pattern is different in this case in comparison with thermal desorption of a surface tungsten oxide (cf. Figs. 3a–3f with desorption sequence Fig. 2 of the paper of Goymour and King (9)). Typical features of aluminum oxide interaction with the (011) plane (lowering of the work function due to the formation of W–O–Al species on this surface) have been observed (Figs. 3c–3f) (cf. Ref. (10)).

After desorption at a temperature $T > 1500$ K the emission pattern starts to resemble the $W–O_{ads}$ system (12) (cf. Figs. 3g and 3h and Figs. 4c and 4d).

Heating to about 1600 K causes further evaporation of tungsten oxide as reported, for example, in Ref. (12).

3.3. *Nitrogen Adsorption*

Nitrogen adsorption at room temperature on bimetallic systems has been studied in this laboratory on (i) a tungsten tip partially covered by palladium (13) and on (ii) oxidized tungsten tips where the palladium and molybdenum islands (clusters) have been deposited (4, 5). In the case of the W–Pd system the work-function change of Pd, due to nitrogen spillover, has been estimated by means of the Fowler–Nordheim plot (13) and the obtained value agreed well with the published data (see quotations in Ref. (13)). In both these cases an ordinary behaviour has been observed, viz., the increase of the work function of Mo, W, and Pd due to chemisorption of nitrogen atoms (in the case of Mo or W directly from the gas phase, in the case of Pd due to nitrogen spillover from Mo or W, respectively). This behaviour agrees with macroscopic measurements [Ref. (13) and citations therein]. The spillover of nitrogen atoms from molybdenum to palladium could be observed if the gap between the metal islands is not broader than about 1 nm (11). However, the tungsten oxide is not commonly used as a support and, moreover, its possible semiconductivity does not totally exclude the influence of an electron transfer from the underlying bulk metal to the supported clusters. The model study on alumina is therefore coming closer to real catalysts.

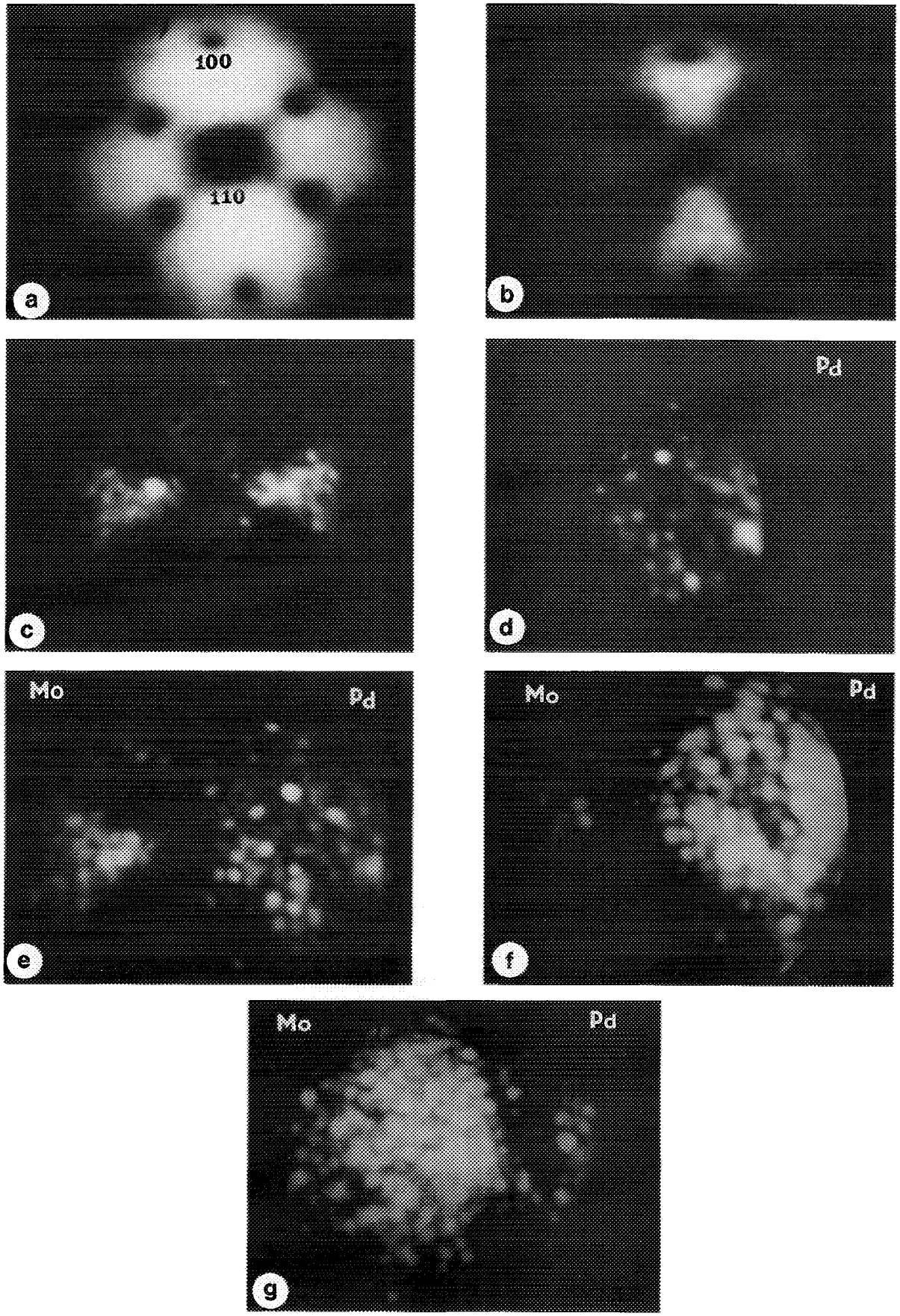

FIG. 2. FEM image of: (a) a clean tungsten surface (image conditions: U = 4.0 kV, T = 300 K); (b) aluminum evaporated onto the tungsten tip (image conditions: U = 4.2 kV, T = 300 K); (c) oxidized aluminum layer (image conditions: U = 5.7 kV, T = 300 K); (d) palladium deposited from the right side (image conditions: U = 4.4 kV, T = 300 K); (e) molybdenum deposited from the left side (image conditions: U = 4.9 kV, T = 300 K); (f) the system heated to 900 K (image conditions: U = 4.9 kV, T = 300 K); and (g) some more molybdenum deposited from the left side (image conditions: U = 4.4 kV, T = 300 K).

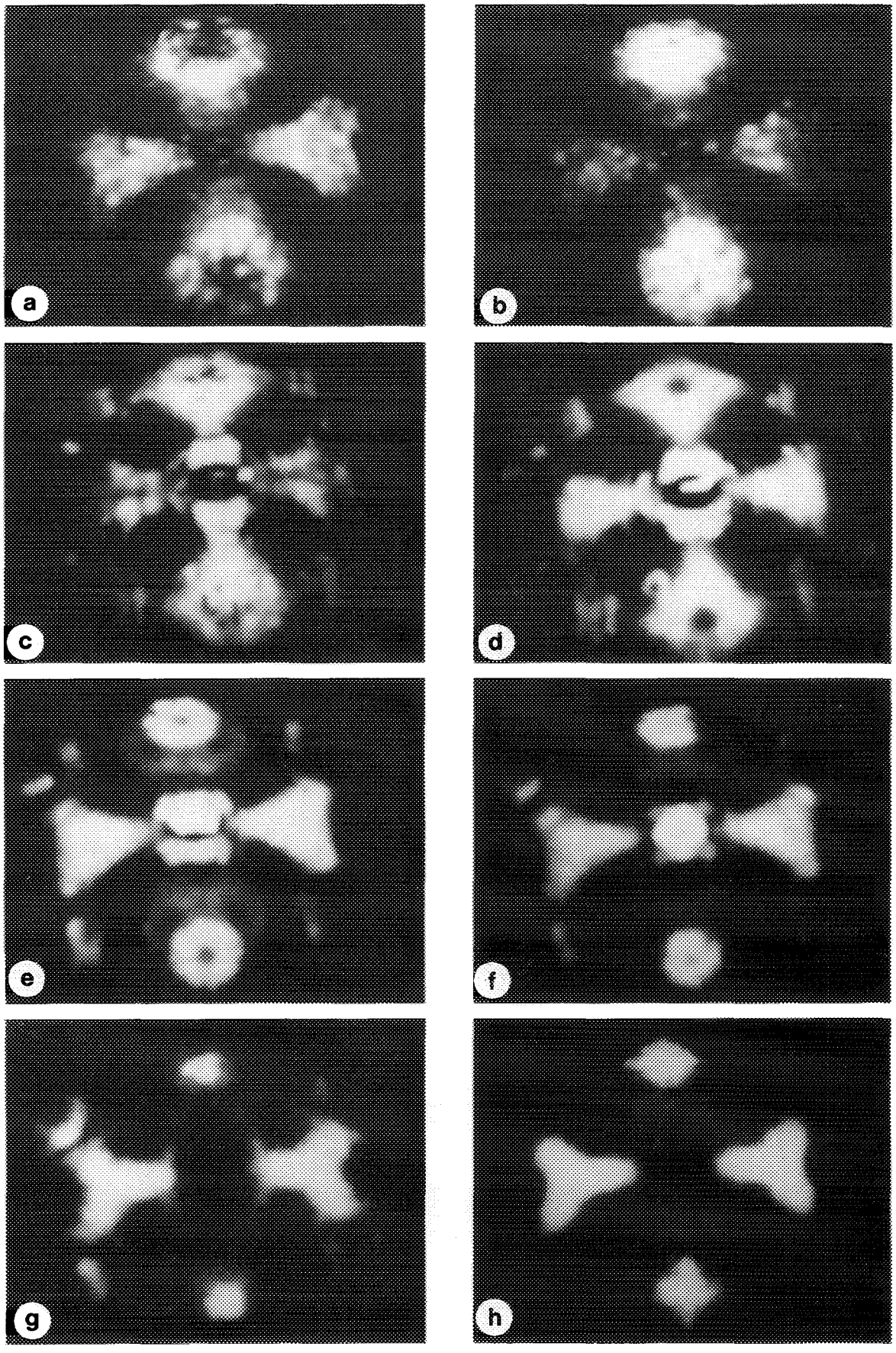

FIG. 3. FEM images of the thermal desorption of alumina layer from the tungsten tip. Alumina layer heated in vacuum to: (a) 1300 K (image conditions: U = 5.5 kV, T = 300 K, I = 0.03 μA); (b) 1350 K (image conditions: U = 5.2 kV, T = 300 K, I = 0.05 μA), (c) to 1400 K (image conditions: U = 5.2 kV, T = 300 K, I = 0.04 μA); (d) 1430 K (image conditions: U = 5.2 kV, T = 300 K, I = 0.04 μA); (e) 1450 K (image conditions: U = 5.1 kV, T = 300 K, I = 0.06 μA); (f) 1450 K (image conditions: U = 4.9 kV, T = 300 K, I = 0.04 μA); (g) 1500 K (image conditions: U = 4.8 kV, T = 300 K, = 0.10 μA); and (h) 1600 K (image conditions: U = 4.7 kV, T = 300 K, I = 0.12 μA).

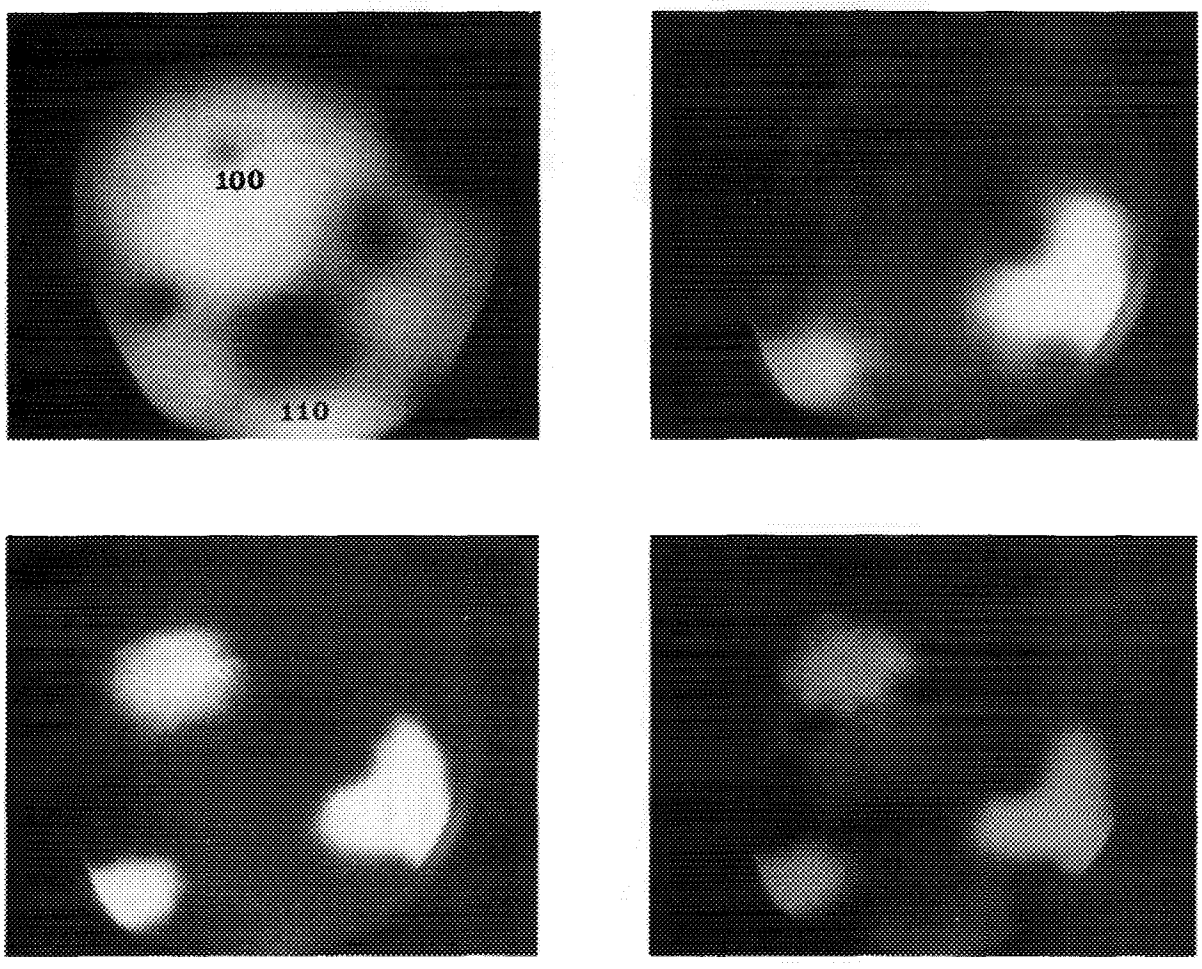

FIG. 4. FEM images of clean tungsten (U = 4.8 kV) (a); tungsten covered by an oxide layer (prepared by O_2 exposure at 78 K, subsequently heated in oxygen to $T \approx 2200$ K (U = 6.2 kV) (b); and after heating the tungsten tip to $T \approx 1300$ K (U = 5.6 kV) (c) and $T \approx 1800$ K (U = 5.6 kV) (d).

A typical result of our experiments is shown in Fig. 5. The Pd–Mo/Al_2O_3 system of Fig. 2 was heated first in vacuo to about 700 K, which is the temperature at which molybdenum already starts to evaporate (Fig. 5a). Figure 5b represents the system after 16 min of exposure to 5×10^{-8} mbar of N_2 at 300 K ($\approx$ 45 L). The negative images taken at a constant voltage and time exposure were digitalized and the photodensity profiles along a chosen line A–B were plotted (Fig. 5c). The photodensity is considered to be proportional to the emission current, thereby giving qualitative information about the work function changes of the particular surface region. The dashed and full curves represent the photodensity profiles of Figs. 5a and 5b, respectively. Comparison of these two curves shows that the work function increases on the molybdenum as well as on the palladium during the nitrogen adsorption. Since at room temperature palladium does not adsorb molecular nitrogen from the gas phase [Ref. (13) and citations therein], the observed work-function increase can be due to the spillover of nitrogen atoms from molybdenum only. The choice of the position of the line A–B crossing the border between the Mo and Pd region is not important. We may note the following:

(i) The changes of the absolute values of the Pd work function depend on the time allowed for the nitrogen migration; the important point, however, is the direction of the change (increase of the work-function) proving the occurrence of the nitrogen spillover to the Pd islands.

(ii) Figure 6 shows results of another experiment, where it is plainly visible that the nitrogen atoms migrate not too far from the border between the regions covered by molybdenum or palladium islands, respectively. Thus under given experimental conditions the emission at the right side of Figs. 5b and 6b is less strongly suppressed than

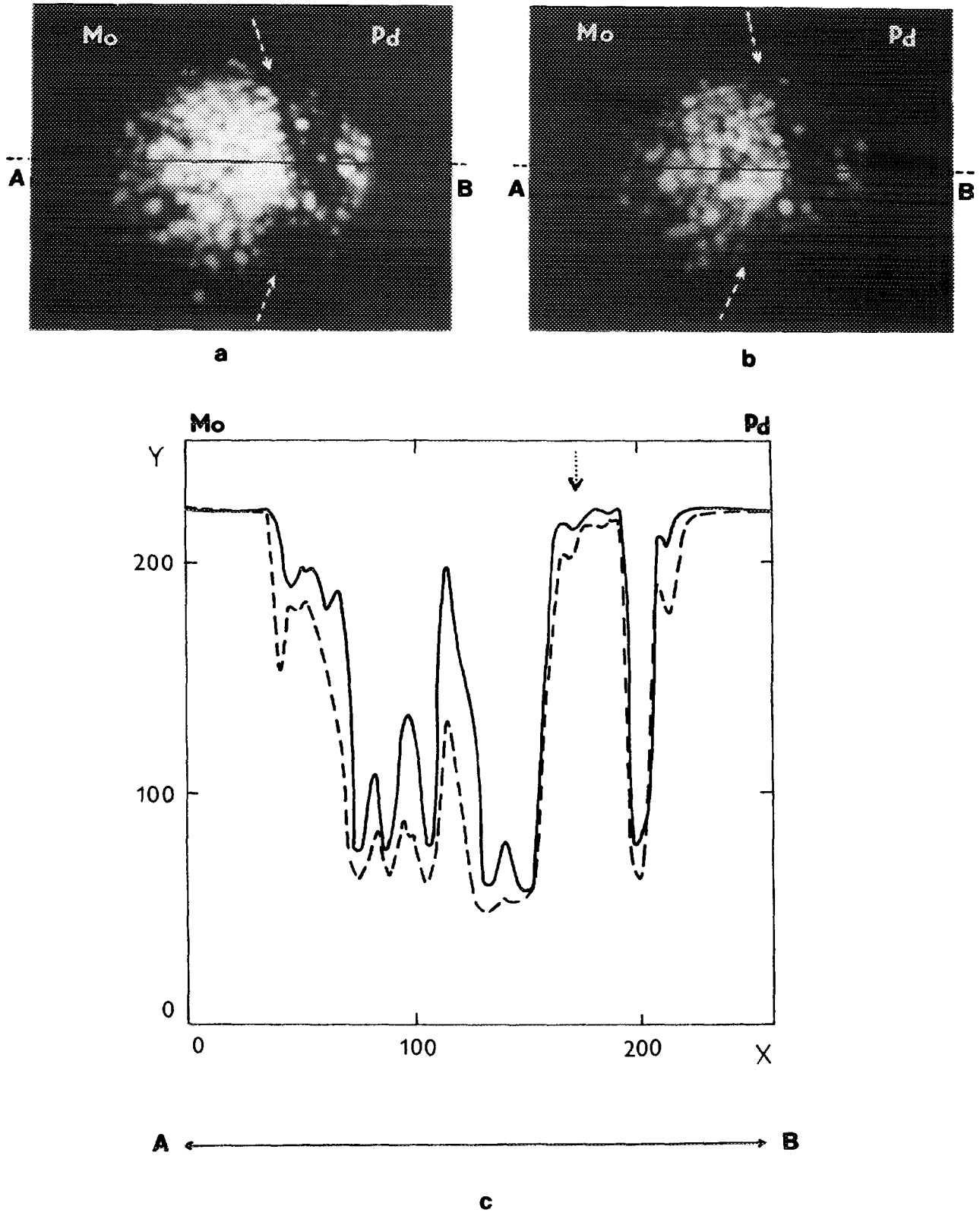

FIG. 5. FEM image of Mo–Pd/Al_2O_3/W system (continuation of Fig. 2g): (a) cleaned by heating in vacuum to 700 K (image conditions: U = 4.4 kV, T = 300 K); (b) after 16 min in 5×10^{-8} mbar of N_2 (image conditions: U = 4.4 kV, T = 300 K); (c) the dashed and full curves correspond to the intensity profiles along the line A–B of Figs. 3a and 3b, respectively. Zero on the y-axis corresponds to the maximum brightness of the image (highest emission, lowest work function) and the value 255 to the zero emission (highest work function). On the x-axis there are positional coordinates along the line A–B in arbitrary units. Arrows show the position of the boundary between the region covered by Mo and Pd clusters, respectively.

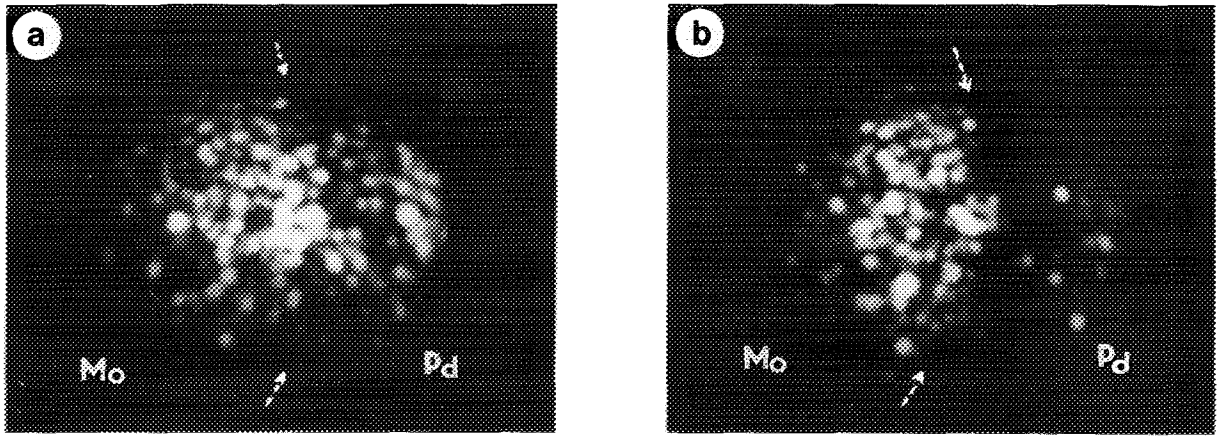

FIG. 6. FEM images of Mo–Pd/Al_2O_3/W system: (a) clean surface (U = 5.1 kV) and (b) after exposure to nitrogen gas (6 Langmuirs) (U = 5.1 kV). Arrows show the position of the boundary between the region covered by Mo and Pd clusters, respectively.

close to the border (obviously due to lower nitrogen coverage there).

CONCLUSIONS

The results presented here have shown that the metal–alumina–metal system can be successfully used for a realistic modeling of supported metal catalysts in field emission microscopy (FEM). It has been shown that FEM, which is a typical surface science technique, limited to a special sample form, can be used for the study of problems related to practical catalysis (e.g., spillover of reactant species) and at the same time the cognitive power of this technique is preserved. As an example, the spillover of nitrogen atoms from molybdenum to palladium islands on alumina was proved.

ACKNOWLEDGMENTS

This work was supported by Grant 44012 of the Academy of Sciences of the Czech Republic. The cooperation of Dr. J. Havel (Institute of Information Theory and Automatization of the Academy of Sciences of the Czech Republic) in the digitalization of FEM images is gratefully acknowledged.

REFERENCES

1. Hudson, J. B., "Surface Science," Butterworth–Heinemann, Boston, 1992.
2. El-Yakhloufi, M. H., and Gillet, E., *Catal. Lett.* **17,** 11 (1993).
3. Foger, K., *in* "Catalysis, Science, and Technology" (J. R. Anderson and M. Boudart, Eds.), Vol. 6, p. 227. Springer-Verlag, Berlin, 1984.
4. Knor, Z., and Šotola, J., *Rev. Roum. Chim.* **34,** 1373 (1989).
5. Knor, Z., and Šotola, J., *Collect. Czech. Chem. Commun.* **53,** 2399 (1988).
6. Chen, P. J., Colaianni, M. L., and Yates, J. T., *Phys. Rev. B* **41,** 8025 (1990).
7. Šotola, J., and Knor, Z., *Appl. Surf. Sci.* **213,** 173 (1988).
8. Knor, Z., and Šotola, J., *Surf. Sci.* **213,** 371 (1989).
9. Goymour, C. G., and King, D. A., *J. Chem. Soc. Faraday Trans.* **68,** 280 (1972).
10. Ross, L. P., and Vanselow, R., *Appl. Phys.* **4,** 161 (1974).
11. Šotola, J., and Knor, Z., *in* "Procedings of The second International Conference on Spillover" (K.-H. Steinberg, Ed.), p. 57. Universität, Leipzig, 1989.
12. Šotola, J., Savkin, V., and Knor, Z., *Collect. Czech. Chem. Commun.* **57,** 2481 (1992).
13. Knor, Z., Edelmann, Ch., Rudny, J., and Stachurski, J., *Appl. Surf. Sci.* **25,** 107 (1986).